

## NUMERICAL INVESTIGATION OF NEAR-WAKE FLOW AND SOUND FIELD OF THE WIND TURBINE WITH W-TYPE TIP STRUCTURE

Baohua LI<sup>1</sup>, Yuanjun DAI<sup>2,\*</sup>, Mingcheng ZHAI<sup>3</sup>, Junhuizhi MA<sup>4</sup>, Zhiying GAO<sup>5</sup>

*In the present study, a new type of wind turbine with a W-type tip structure blade is designed. In order to explore the characteristics of the flow field and the sound wave propagation in the near wake region of the wind turbine with W-type tip structure, large-eddy simulation (LES) and the Kirchhoff Ffowcs Williams-Hawkins (KFW-H) equation are coupled. Obtained results show that the W-type tip structure of the wind turbine improves the velocity distribution near the blade tip. Meanwhile, this tip structure decreases the vorticity value at the blade tip by 20.9% - 28.68%. It is found that the W-type tip structure reduces the peak value of the natural frequency and the corresponding harmonics. Moreover, it reduces the maximum value of the sound pressure level by 2.98% - 4.85%.*

**Keywords:** wind turbine, W-type tip structure, numerical simulation, sound pressure level

### 1. Introduction

The “low-carbon” concept has been increasingly become the development strategy in the world. Accordingly, exploiting the clean energy, including the wind power, has been quickly developed in the past few years. Reviewing the literature indicates that the majority of investigations in the field of wind power

<sup>1</sup> Prof., College of Mechanical Engineering, Shanghai DianJi University, China, e-mail:764500870@qq.com

<sup>2</sup> Prof., College of Mechanical Engineering, Shanghai DianJi University, China, e-mail:24354267@qq.com

<sup>3</sup> M. S., College of Mechanical and Electrical Engineering, Xinjiang Agricultural University, China, e-mail:756959147@qq.com

<sup>4</sup> M. S., College of Mechanical and Electrical Engineering, Xinjiang Agricultural University, China, e-mail:475136164@qq.com

<sup>5</sup> Prof., College of Energy Engineering, Xinjiang Institute of Engineering, China, e-mail: hawkwarm@imut.edu.cn

\*Corresponding Author: Yuanjun Dai, 24354267@qq.com

technology are focused on how to improve the output performance of the wind turbine. Studies show that although most modern wind turbines meet the expected output performance, generated noises from a wind turbine are a challenging issue. These noises are mainly generated by the yaw system, tower disturbance, tip vortex, trailing edge vortex, and the boundary layer separation. It was found that among these noise sources, the tip vortex and trailing edge vortex have the highest share in the noise generation <sup>[1]-[4]</sup>. Accordingly, the present study is mainly focused on reducing the vortex noise of the wind turbine through a modified airfoil trailing edge <sup>[5]</sup>.

In recent years, many scholars performed numerical and experimental investigations on this topic and showed that for a certain Reynolds numbers, broadband noise of the wind turbine can be reduced by porous airfoils and airfoil trailing edge serrations and brushes.

Bohn <sup>[6]</sup> used porous airfoils and then measured the sound field of the wind turbine. He found that porous airfoils can effectively suppress the noise. Moreover, Howe <sup>[7]-[8]</sup> studied the theory of noise reduction for a wind turbine with airfoil trailing edge serrations and pointed out that it can effectively reduce noise at high frequencies when the feature size is much smaller than the geometry size of the serrations. Some scholars mounted small auxiliary wings, called tip vanes, on the tip of turbine blades. It is worth noting that this idea is originated from the aircraft wing design. More specifically, Van Holten <sup>[9]</sup> proposed mounting tip vanes on the tip of turbine blades. Chuichi Arakawa <sup>[10]-[11]</sup> performed a compressible large-eddy simulation (LES) and showed that the sound pressure level in the high-frequency domain decreases for the ogee type tip shape. Wang Jianwen and Dai Yuanjun <sup>[12]-[15]</sup> studied the aerodynamic performance and noise production of the wind turbine with different extra tip vanes. The results showed that installing extra tip vanes can effectively reduce noise.

Most recently, Dai <sup>[16]</sup> carried out the numerical simulation to investigate the flow field in the near wake region of the wind turbine. It should be indicated that the established wind turbine model, division of grids, setting of the calculation parameters, analysis methods and the calculation results have certain guiding significance for the present study. In this paper, it is intended to conduct CFD simulations to investigate the flow field and sound pressure level of the wind turbines with a W-shaped blade tip at working conditions. To this end, the compressible large-eddy simulation (LES) will be carried out for a three-dimensional flow field and the sound source integral plane defined by the

Kirchhoff-Ffowcs Williams Hawkings (K-FWH) equation will be solved to obtain the acoustic radiation characteristics.

## 2. Physical model and unsteady calculation

### 2.1 Physical model

In this section, the S-series airfoil is installed on the straight blade vertical axis wind turbine (SB-VAWT). It is worth noting that the S-series airfoil is a special airfoil with superior characteristics, which is developed for wind turbine blades. Studies show that the S-series airfoil can correct the aerodynamic defects of the conventional airfoil and improve the aerodynamic performance of the wind turbine impeller. The parameters of the wind turbine are presented in Table 1.

Table 1 Parameters of the wind turbine

| Blade parameter     | Value   |
|---------------------|---------|
| Number of blades    | 3       |
| Blade length        | 0.7 m   |
| Tip chord length    | 0.04 m  |
| Aspect ratio        | 4.22    |
| Twist angle         | 5.8 °   |
| Rated wind speed    | 8 m/s   |
| Start-up wind speed | 3.1m/s  |
| Rated speed         | 750 rpm |

In the present study, two W-type tip structure blades with different sizes are designed for wind turbines by the orthogonal test. Table 2 presents the geometric parameters of the W-type tip structure blade. Furthermore, figure 1 shows the structural sketch of the W-type tip structure blade.

Table 2 Parameters of the W-type tip structure blade

| Name    | Height(h) | Opening angle( $\theta$ ) | Width(a) |
|---------|-----------|---------------------------|----------|
| W1-type | 25mm      | 60°                       | 14mm     |
| W2-type | 54mm      | 20°                       | 14mm     |

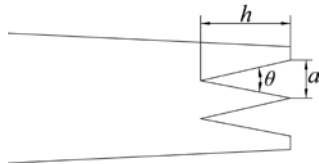


Fig. 1. Structural sketch of the W-type tip structure blade

A suitable spatial three-dimensional coordinate system was selected by the Unigraphics NX software. It is assumed that the incoming wind is along the positive direction of the X-axis so that the Y- and Z-axes are perpendicular to the wind. Figures 2 and 3 illustrate the model of the non-modified (conventional) and the modified wind turbine models, respectively. It should be indicated that the W-type tip structure blade (hereinafter called W-type tip wind turbine) is installed in the modified model.

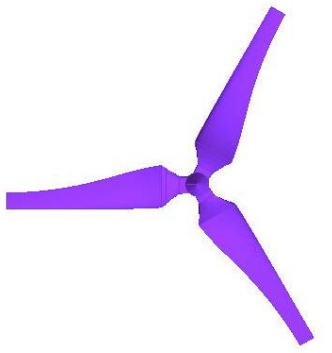


Fig. 2. Configuration of the non-modified (conventional) wind turbine rotor

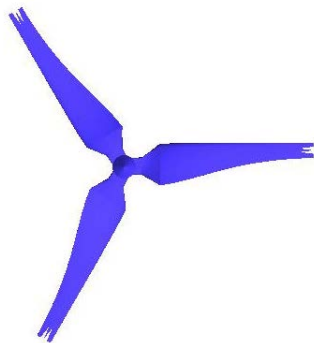


Fig. 3. Configuration of the W-type tip wind turbine rotor

## 2.2 Mesh generation

In order to achieve higher calculation accuracy and reduce the computational expense, the fluid region is divided into three parts, including the rotating fluid region near the wind wheel, internal flow field region, and the external flow field region. In order to obtain more accurate results, high mesh density is considered in the rotating and the internal flow field regions.

Considering the complex spatial surface of blades and characteristics of the flow field, unstructured tetrahedral meshes and interval sizes are defined through sizing functions. Figure 4 shows the generated meshes in the computational domain. It is observed that as the distance to the rotor increases, the interval sizes increase too. The numbers of cells in the rotor and the rotating

region is around  $203 \times 104$ , while that in the external flow field region is about  $62 \times 104$ .

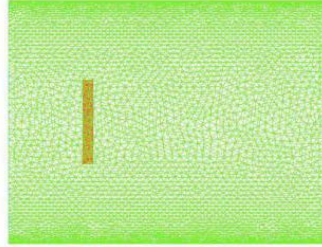


Fig. 4. Generated mesh in the computational domain

## 2.3 Calculation conditions

### 2.3.1 Turbulence model and solver setting

The fluid flow on the surface can be regarded as the flow with low speed. The mean speed of the airflow in the computational domain is less than 8 m/s so that the Mach number is about 0.023, which is much less than 0.3. Accordingly, the fluid compressibility can be ignored. The pressure-based solver is selected for the simulation and the energy equation is not considered. The flow field on the wind turbine is unsteady and the pressure fluctuates so that a transient simulation should be performed. Moreover, an appropriate turbulence model is selected and the Smagorinsky-lily model is set to fit sub-grid scales in the large eddy simulation (LES). The PISO algorithm is applied to solve the Navier-Stokes equations. In order to obtain a more accurate result, the momentum equation is solved through the second-order central difference scheme.

### 2.3.2 Boundary conditions

The boundary conditions and initial conditions are called the solution conditions. It means that to get a unique solution for the flow field, the boundary conditions should be separately set in the calculation.

Boundaries of the computational domain consist of the inlet and outlet boundaries, the rotating region and some key interfaces. The velocity inflow boundary conditions are used at the inflow boundary and the velocity is set to 8 m/s. In order to avoid the disturbance in the fluid and sound field, which is generated by the stern-rudder, it is assumed that the rotor is opposite to the wind tunnel center, while the stern-rudder is fixed. Moreover, the wind flows along the x-direction, the outlet boundary is the pressure-outlet and the outlet pressure is

atmospheric. The flow field is divided into a rotating and a stationary region. The Rotating region is simulated by a moving reference frame (MRF), which rotates at 750 rpm. To successfully invoke and exchange data between the rotating and stationary regions, an interface is defined between the internal and external flow fields. Interface between internal and external flow fields is computed by Interface. Furthermore, the rotor is considered as a moving wall, which rotates around the x-axis. It is assumed that the relative speed between the fluid and the rotor is zero.

### 2.3.3 Sound field solver

The sub-relaxation factor of each flow parameter of the sound field is the same as that for the flow field. The time step is set to 0.00222s. Studies show that the flow field in the computational domain becomes stable after six spins of the tower [17]. Accordingly, the sound data is extracted after twelve spinning's of the tower.

## 3. Numerical simulation of the flow field

The numerical simulation and analysis of the flow field of original and W-type blades are carried out with the same solver and initial conditions. The rotating direction of the rotor during the simulation is counterclockwise.

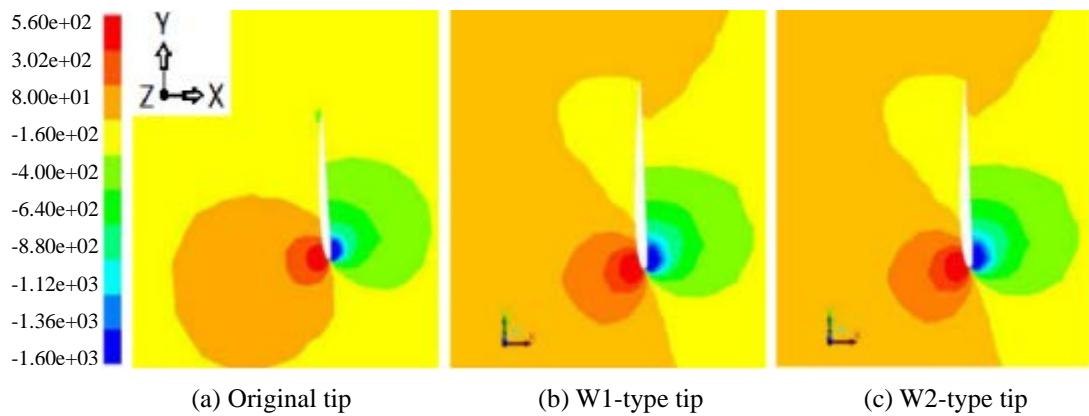


Fig. 5. Static pressure distributions of the wind turbine with different tip vanes at  $X/R = 0.08$

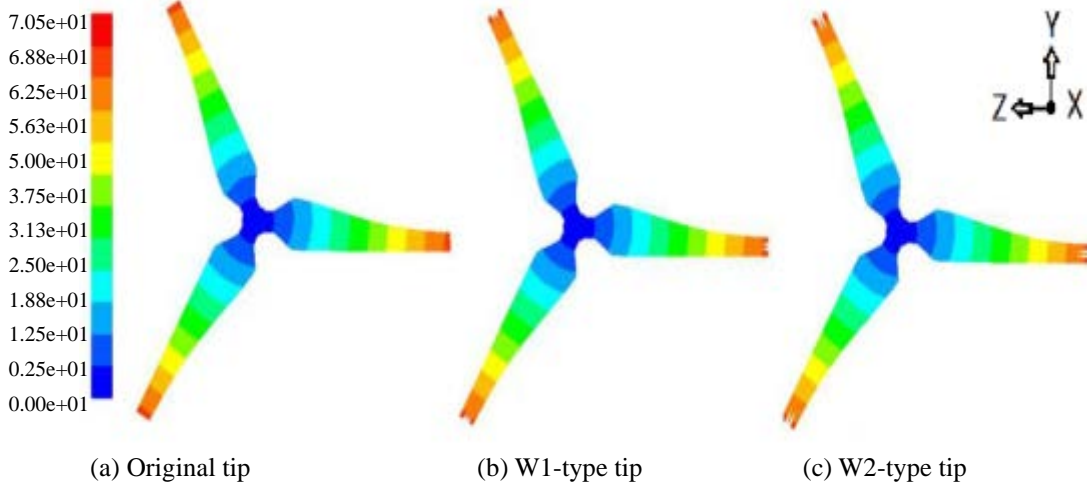


Fig. 6. Velocity distributions of the wind turbine with different tip vanes

Figure 6 illustrates the pressure distribution of the wind turbine with different tip vanes at  $X/R=0.08$ , where  $X$  and  $R$  denote the distance to the origin and the rotor radius, respectively. It is observed that the pressure near the front edge is much bigger than that of the opposite edge, and there is an area with negative pressure at the back edge of the original blade. Meanwhile, it is found that the distribution of negative static pressure is more dispersed on the suction surface. Figure 5 indicates that the back edge of the original blade forms a negative pressure area on the pressure surface. Since the wing flow increases as the tip height ( $h$ ) increases, the negative pressure of the back edge decreases. Meanwhile, the positive pressure of the front surface increases, indicating that the disturbance action of the tip vortex reduces. According to Bernoulli's principle, the velocity at the pressure surface of the blade is much bigger than that at the suction surface, indicating that the suction surface is affected by the vortex.

Figure 6 presents the velocity distribution of the rotor before and after the modification. It is observed that the flow velocity increases from the blade root to its tip and the tip has the fastest velocity. The maximum velocity of the original rotor is 80.3 m/s, while those of the W1-type and W2-type tips are 77.1 m/s and 75.53 m/s, respectively. It is found that the peak velocity of the rotor with a W-shaped tip decreases slightly and the maximum velocity of W1-type tip and W2-type tip decreased by 3.99 % and 5.94 %, respectively.

The pressure of the windward side is much higher than that of the leeward side. This is especially more pronounced at the tip region. The high-pressure

airflow from the windward side goes around the tip to the leeward side so that a vortex is formed.

Figure 7 illustrates the velocity vector distribution of the wind turbine with different tip vanes. Comparing the velocity vector between the original tip and W-type tip shows that disturbance on the suction surface of the original blade at the trailing edge is greater than that of the W-type tip.

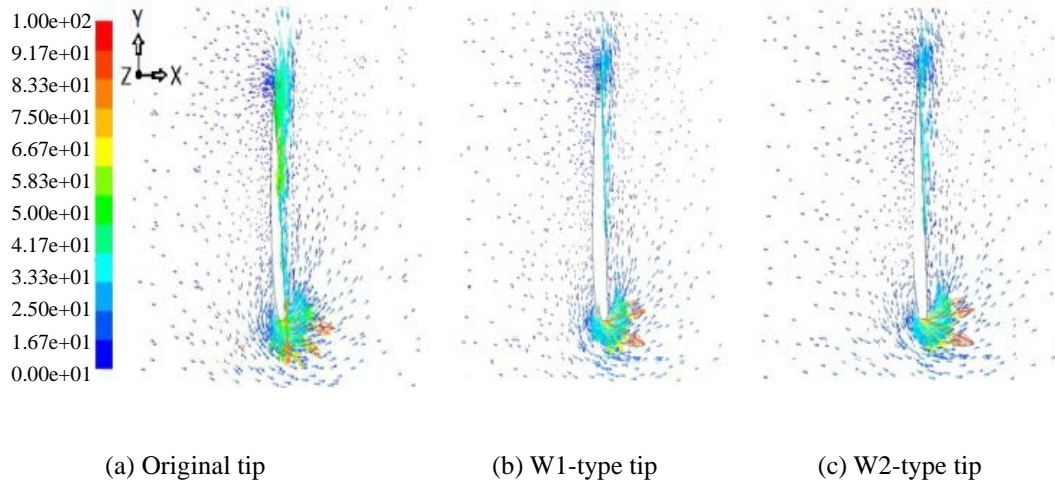


Fig. 7. Speed vector distribution of the wind turbine with different tip vanes at  $X/R = 0.08$

In this part, it is intended to analyze the vorticity distribution on the plane  $X=0$ , where  $X$  is the distance to the origin. Because the plane  $X=0$  is in the rotating region and it is closely linked to the rotor. The fluid velocity, pressure and vorticity have maximum variation in the rotating region, especially at the blade surface and the tip region. It should be indicated that the vorticity is one of the key parameters for both flow and acoustic fields.

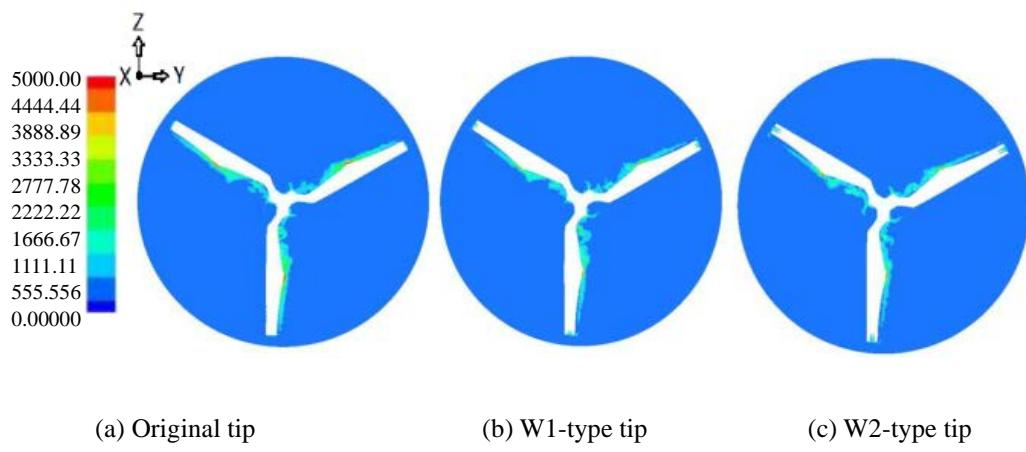


Fig. 8. Vortex distribution of the wind turbine with different tip vanes at  $X=0$

Figure 8 shows the vorticity distribution of the wind turbine with different tip vanes at  $X=0$  plane. The tip vortex is attached to the trailing edge. Comparing the vorticity fields of the original and W-type tip shows that the W-type tip structure can reduce the vorticity. Average vorticity of the original, W1-type tip and W2-type tip rotor at plane  $X=0$  are  $287.19\text{s}^{-1}$ ,  $227.16\text{s}^{-1}$  and  $204.81\text{s}^{-1}$ , respectively. It is concluded that mounting the W-type tip can reduce the average vorticity at plane  $X=0$ . Obtained results show that W1-type and W2-type tip rotors can reduce the vorticity by 20.9 % and 28.68 %, respectively.

#### 4. Numerical simulation of the sound field

In order to investigate the influence of the W-type tip on the aerodynamic noise, a rotating plane is considered, which is perpendicular to the flow direction and passes the tip's leading edge. The rotation center is set as the origin and the wind slows along the X-axis. Figure 9 illustrates the distribution of the measuring points on the plate.

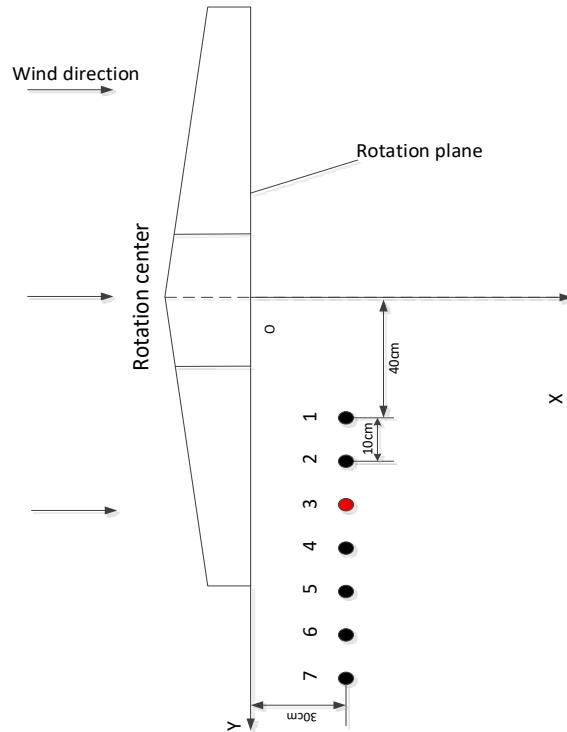


Fig. 9. Distribution of the measuring points

Figure 10 presents the noise spectrum for different tip vanes at point 3. The position and rotating angle of point 3 are  $(30, -60, 0)$  and  $90^\circ$ , respectively.

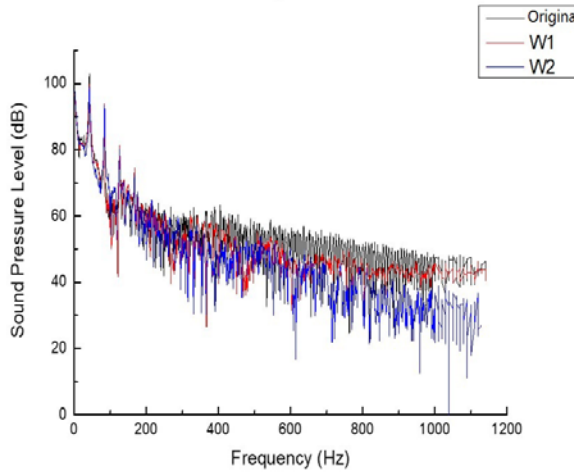


Fig. 10. Noise spectrum for different tip vanes at point3

Based on the equation of the blade passing frequency (BPF), the rotating frequency of the rotor is 37.5 Hz. Figure 10 shows that the peak values of these three wind turbines with different tip structures in the spectrogram are at 37.5 Hz or frequencies which are integer multiples of the natural frequency. The peak values of sound pressure level (SPL) in the natural frequency and its harmonics are 103dB, 100dB and 98dB. It is found that the noise in the natural frequency of the W1-type rotor decreases by 2.98 %, while that of W2-type decreases by 4.85 %. Moreover, it is observed that as the tip height (h) increases, the peak value of SPL in the natural frequency of the wind turbine and its harmonics decreases. This is in excellent consistency with the experimental results published by Dai's research group [18].

## 5. Conclusion

In the present study, the flow and sound field of the fluid and the vertex noise from different tip shapes are numerically investigated. The tip speed ratio is set to  $\lambda=6.8$  and the FW-H equation is solved in the LES solver. Based on the obtained results and findings, the following conclusions can be drawn:

1) The back edge of the original blade forms a negative pressure area on the pressure surface, which originates from the wing flow. It is found that as the tip height (h) increases, the negative pressure of the back edge decreases. Meanwhile, the positive pressure of the front surface increases, indicating that the disturbance of the tip vortex reduces. It is found that the suction surface is more affected by the vortex.

2) Velocity distributions of rotors with different tip shapes are similar and the W-type tip can reduce the maximum speed slightly. Comparing the velocity vector distributions showed that the largest disturbances on the rear edge of the suction surface from high to low belong to the non-modified wind turbine, a wind turbine with W1-type tip and the wind turbine with W2-type tip. It is concluded that as the tip height (h) increases, the tip vortex strength decreases.

3) Tip vortex is installed on the trailing edge. Comparing the vorticity fields between the original tip and W-type tip shows that the W-type tip structure can reduce the vorticity.

4) Obtained results show that as the tip height (h) increases, the peak value of SPL in the natural frequency of the wind turbine and its harmonics decreases. The noise level in the natural frequency of W1- and W2-type tip rotors decreases by 2.98 % and 4.85 %, respectively.

5) From the technical and practical point of view, the design idea of W-shaped wind turbine blade is to reduce the tip vortex strength and tip pressure difference, so as to reduce the tip noise of wind turbine under the condition of almost constant output power. Therefore, the W-shaped structure provides a reference for the design of wind turbine.

### Acknowledgements

This work was supported by the National Natural Science Foundation Project (Grant No. 51966018, 51466015), the Xinjiang Outstanding Young Scientific and Technological Talents Project (Grant No. 2017Q036), the Xinjiang Tianshan Talent Project (Grant No. 2018xgjtsyc2-1-5)

### R E F E R E N C E S

- [1]. S. Sun, F. Liu, S. Xue, “Review on wind power development in China: Current situation and improvement strategies to realize future development”, in Renewable and Sustainable Energy Reviews, **vol.45**, Dec. 2015, pp. 589-599
- [2]. G. Z. Wang, X. L. Li, J. X. Zhang, W. J. Huang, “Experimental Study on the Noise Sources Generation Mechanism of Large Wind Turbine”, in Piezoelectrics & Acoustooptics, **vol.38**, no. 5, May 2016, pp. 829-832
- [3]. S. Oerlemans, P. Sijtsma, B. Mendez-Lopez B, “Location and quantification of noise sources on a wind turbine”, in Journal of Sound and Vibration, **vol. 299**, no. 4-5, Apr. 2007, pp. 869-883
- [4]. J. W. Wang, R. B. Jia, K. Q. Wu, “Numerical Simulation on Effects of Pressure Distribution of Wind Turbine Blade with a Tip Vane”, in An International Journal of Thermal and Fluid Sciences, **vol. 16**, no. 3, Mar. 2007, pp. 203-207

- [5]. *W. Y. Liu*, “A review on wind turbine noise mechanism and de-noising techniques. *Renewable Energy*”, **vol. 108**, Dec. 2017, pp. 311-320
- [6]. *A. J. Bohn*, “Edge noise attenuation by porous-edge extensions”, in AIAA paper, Dec. 1976, pp. 80
- [7]. *M. Howe*, “Aerodynamic Noise Of A Serrated Trailing Edge”, in *Journal Of Fluids And Structures*, **vol. 5**, no. 1, Jan. 1991, pp. 33-45
- [8]. *M. Howe*, “Noise Produced By A Sawtooth Trailing Edge”, in *The Journal Of The Acoustical Society Of America*, **vol. 90**, Dec. 1991, pp. 482
- [9]. *B. De Wit, J.W. Van Holten, A. Van Proeyen*, “Transformation rules of supergravity multiplets”, in *Nuclear Physics B*, **vol. 167**, no. 1, Jan. 1980, pp. 186-204
- [10]. *O. Fleig, C. Arakawa*, “Numerical simulation of wind turbine tip noise”, in *America: American Society of Mechanical Engineers*, Dec. 2004, pp. 1190
- [11]. *C. Arakawa, O. Fleig, M. Iida*, “Numerical Approach for Noise Reduction of Wind Turbine Blade Tip with Earth Simulator”, in *Journal of the Earth Simulator*, **vol. 2**, no. 3, Mar. 2005, pp. 11-33
- [12]. *J. W. Wang, R. B. Jia, K. Q. Wu*, “Effect of a Tip Vane on Pressure Distribution of Wind Turbine Blade”, in *Journal of Engineering Thermophysics*, **vol. 25**, no. 5, May. 2006, pp. 760-762
- [13]. *L. R. Zhang, J. W. Wang, L. Qu*, “Three-Dimensional Numerical Simulation of Flow Field of Wind Turbine with and without Tip Vane”, in *Acta Energiae Solaris Sinica*, **vol. 32**, no. 11, Nov. 2011, pp. 1599-1064
- [14]. *L. R. Zhang, J. W. Wang, H. P. Yu*, “Research on Characteristics of the Flow Field of Wind Turbine With the S-Type Tip Vane”, in *Journal of Engineering Thermophysics*, **vol. 33**, no. 5, May. 2012, pp. 788-791
- [15]. *Y. J. Dai, J. W. Wang, W. M. Wu*, “Numerical Calculation Analysis of Blade Tip Near Wake Region of S Series New Airfoil Wind Turbine”, in *Acta Energiae Solaris Sinica*, **vol. 5**, no. 2, Feb. 2014, pp. 195-201
- [16]. *Y. J. Dai, B. H. Li*, “A numerical study of the acoustic radiation characteristics of the aerodynamic noise in the near-wake region of a wind turbine”, in *Results in Physics*, **vol. 15**, Dec. 2019, 102782
- [17]. *Y. J. Dai, C. Z. Ren, B. H. Li*, “Numerical Simulation of Effect of V-Type Blade Tip Structure on Aerodynamic Noise at Tip Region of Wind Turbine”, in *Chin Measur Test Technol*, **vol. 43**, no. 7, Jul. 2017, pp. 128-133
- [18]. *Y. J. Dai, C. Z. Ren, L. J. Xu*, “Experimental Study of Effect of V-Type Blade Tip Structure on Aerodynamic Noise at Tip Region of Wind Turbine”, in *Acta Energiae Solaris Sinica*, **vol. 38**, no. 2, Feb. 2017, pp. 472-477.